



## RESEARCH ARTICLE

# Anticancer properties of erucin, an H<sub>2</sub>S-releasing isothiocyanate, on human pancreatic adenocarcinoma cells (AsPC-1)

Valentina Citi<sup>1</sup> | Eugenia Piragine<sup>1</sup> | Eleonora Pagnotta<sup>2</sup> | Luisa Ugolini<sup>2</sup> |  
Lorenzo Di Cesare Mannelli<sup>3</sup>  | Lara Testai<sup>1,4</sup> | Carla Ghelardini<sup>3</sup> | Luca Lazzeri<sup>2</sup> |  
Vincenzo Calderone<sup>1,4,5\*</sup> | Alma Martelli<sup>1,4\*</sup> 

<sup>1</sup>Department of Pharmacy, University of Pisa, Pisa, Italy

<sup>2</sup>Council for Agricultural Research and Economics, Research Centre for Cereal and Industrial Crops, Bologna, Italy

<sup>3</sup>Department of Neuroscience, Psychology, Drug Research and Child Health – NEUROFARBA – Section of Pharmacology and Toxicology, Florence, Italy

<sup>4</sup>Interdepartmental Research Centre “Nutraceuticals and Food for Health (NUTRAFOOD)”, University of Pisa, Pisa, Italy

<sup>5</sup>Interdepartmental Research Centre of Ageing Biology and Pathology, University of Pisa, Pisa, Italy

## Correspondence

A. Martelli, Department of Pharmacy, University of Pisa, via Bonanno 6, 56126 Pisa, Italy.

Email: alma.martelli@unipi.it

## Funding information

MiPAAF (D.M. 2419, 20/02/08), Grant/Award Number: Part of the work (isolation of natural erucin) has

Plants of the *Brassicaceae* family are well-known for containing the glucosinolate myrosinase system, which is able to release isothiocyanates after plant biotic and abiotic lesions. Erucin (ERU; 1-isothiocyanato-4-(methylthio)-butane), an isothiocyanate particularly abundant in arugula (*Eruca sativa* Mill., *Eruca vesicaria* L., etc.), derives from the hydrolysis of the glucosinolate glucoerucin by the enzyme myrosinase. Many other natural isothiocyanates influence cancer cells and, in particular, induce antiproliferative effects at relatively high concentrations. Similar antiproliferative effects have also been shown by the newly emerging gasotransmitter hydrogen sulfide (H<sub>2</sub>S) and by H<sub>2</sub>S-releasing compounds. In a previous study, our group demonstrated that isothiocyanates release H<sub>2</sub>S in biological environments. In this work, we demonstrated the H<sub>2</sub>S-donor properties of ERU in pancreatic adenocarcinoma cells (AsPC-1) and delineated its profile as a chemopreventive or anticancer agent. Indeed, ERU showed significant antiproliferative effects: ERU inhibited AsPC-1 cell viability at relatively high concentrations (30–100 μM). Moreover, ERU inhibited cell migration, altered the AsPC-1 cell cycle, and exhibited proapoptotic effects. Finally, ERU inhibited ERK1/2 phosphorylation. This mechanism is particularly important in AsPC-1 cells because they are characterized by a mutation in KRAS that determines KRAS hyperactivation followed by MAP-kinase hyperphosphorylation, which plays a pivotal role in pancreatic cancer proliferation, growth, and survival.

## KEYWORDS

AsPC-1, erucin, hydrogen sulfide, isothiocyanates, pancreatic cancer

## 1 | INTRODUCTION

In recent years, the anticancer properties of dietary agents have been widely investigated, and in particular, it has been

demonstrated that the consumption of Brassicaceae vegetables (crucifers), such as broccoli, cauliflower, cabbage, and rocket salad, is associated with a lower risk of cancer (Fofaria, Ranjan, Kim, & Srivastava, 2015).

**Abbreviations:** AsPC-1, pancreatic adenocarcinoma cells; AUC, area under the curve; BITC, benzyl isothiocyanate; DADS, diallyl disulfide; DATS, diallyl trisulfide; DMSO, dimethyl sulfoxide; ERK, extracellular-signal-regulated kinase; ERU, erucin; FBS, foetal bovine serum; FI, fluorescence index; ITCs, isothiocyanates; MAPK, mitogen-activate protein kinase; PBS, phosphate buffer solution; PEITC, phenethyl isothiocyanate; RPMI, Roswell Park Memorial Institute; SFN, sulforaphane; U, myrosinase unit; WSP-1, Washington State Probe-1; WST, water-soluble tetrazolium salt

\*These authors equally contributed to the work

These edible plants contain high amounts of isothiocyanates (ITCs), which are produced through the enzymatic hydrolysis of glucosinolates by endogenous myrosinase and exhibit antiproliferative activity against cancer in both cell culture and animal models (Nastruzzi et al., 2000).

In fact, some natural ITCs, such as sulforaphane (SFN), phenethyl isothiocyanate, benzyl isothiocyanate (BITC), and erucin (ERU) derive from *Brassicaceae* plants and have inhibitory effects on the growth of several types of cultured cancer cells, including leukaemia, prostate cancer, breast cancer, lung cancer, cervical cancer, and colorectal cancer. Moreover, ITCs are well absorbed and highly bioavailable, making them promising compounds for anticancer therapies (Fofaria et al., 2015).

Many studies have demonstrated that ITCs exert anticancer effects through different mechanisms of action, including promoting cell cycle arrest and apoptosis, interacting with the Keap1-Nrf2-ARE pathway and upregulating phase II detoxification enzymes (Fuentes, Paredes-Gonzalez, & Kong, 2015).

SFN is the most studied isothiocyanate in *Brassicaceae* vegetables and has been particularly studied in broccoli and broccoli sprouts (Clarke et al., 2011). However, ERU, an isothiocyanate structurally related to SFN and typically present in high amounts in wild rocket (*Eruca sativa* Mill.), is still less studied. ERU is produced from its precursor, the glucosinolate glucoerucin, by the plant enzyme myrosinase; a myrosinase-like thioglucosidase activity has been recognized in the bacteria of the human gut. Notably, ERU is also produced in the human body after the biotransformation of SFN through the reduction of the sulfur atom (Melchini & Traka, 2010).

Recently, our group described some synthetic aryl isothiocyanates as H<sub>2</sub>S-donor agents, exhibiting significant effects on the cardiovascular system, attributable to the donation of H<sub>2</sub>S (Martelli et al., 2014).

Aside from these synthetic compounds, other natural ITCs, such as allyl isothiocyanate, which is highly present in black mustard (*Brassica nigra* L.), 4-hydroxybenzyl isothiocyanate, which is highly present in white mustard (*Sinapis alba* L.), benzyl isothiocyanate, which is highly present in garden cress (*Lepidium sativum* L.), SFN, and ERU have also been described as slow H<sub>2</sub>S-releasing compounds (Citi et al., 2014; Lucarini et al., 2018).

H<sub>2</sub>S is a well-known endogenous gasotransmitter that plays pivotal roles in the cardiovascular system and respiratory system and in regulating cell growth. Recent studies have indicated that H<sub>2</sub>S has two opposite effects on cancer cell growth that may be due to the concentration of H<sub>2</sub>S and the time of exposure to cancer cells. This behaviour, defined as "hormetic," has been confirmed in different studies reporting that endogenous H<sub>2</sub>S, as well as the exposure to low levels of exogenous H<sub>2</sub>S or H<sub>2</sub>S-donors for a short duration, could have antiapoptotic effects in cancer cells, promoting and maintaining cancer growth (Hellmich, Coletta, Chao, & Szabo, 2015). In contrast, treatment with a relatively high concentration of H<sub>2</sub>S-donors for a long time has been reported to inhibit cancer cell growth in different types of tumours, thus indicating that slow-releasing H<sub>2</sub>S donors could be an innovative and promising therapeutic strategy in antineoplastic therapy (Calderone, Martelli, Testai, Citi, & Breschi, 2016).

Interestingly, there is an intriguing overlap between many anticancer effects attributed to some ITCs and those exhibited by treatments with some known H<sub>2</sub>S donors (De Cicco et al., 2017; Panza et al., 2015).

Among the several types of cancer, pancreatic adenocarcinoma is one of the most lethal forms, and although substantial progress has been made in understanding the biology of this cancer, it still has an extremely poor prognosis.

For this reason, in this paper, the AsPC-1 human pancreatic adenocarcinoma cell line was selected. AsPC-1 cells are particularly aggressive due to their molecular and genetic status; in fact, they are characterized by the lack of the LKB1 tumour suppressor protein causing a particular resistance to apoptosis and by homozygote mutations in the *KRAS* gene, promoting the constitutive activation of this kinase (Deer et al., 2010). On this basis, in this study, we focused our attention on the anticancer effects of ERU, a natural isothiocyanate with H<sub>2</sub>S donor properties, to investigate the following primary endpoints: its ability to enter AsPC-1 cells and to release H<sub>2</sub>S at the intracellular level, its capacity to inhibit cell viability and migration, its ability to alter the AsPC-1 basal cell cycle, and its ability to exert proapoptotic effects. Finally, a possible mechanism of action was investigated to evaluate the involvement of the MAPK/ERK pathway in the anticancer properties of ERU.

## 2 | MATERIALS AND METHODS

### 2.1 | Isolation of natural ERU

Erucin was produced from natural glucoerucin by myrosinase-catalysed hydrolysis. The glucosinolate was purified from *E. sativa* Mill. seeds stored in the *Brassicaceae* collection at CREA-CI, Bologna, Italy (Lazzeri et al., 2013). Glucoerucin was isolated as K<sup>+</sup> salts from defatted seed meal via extraction with boiling 70% ethanol followed by ion exchange chromatography and gel filtration chromatography, as described previously (Franco et al., 2016). Isolated glucoerucin was analysed by HPLC-UV after enzymatic desulfation according to the ISO 9167-1 method, yielding 99% purity based on the peak area value and 96% purity based on weight. Myrosinase, 36 U/ml, was isolated from ripe seeds of white mustard (*S. alba* L.) as previously reported (Pessina, Thomas, Palmieri, & Luisi, 1990) and stored at 4°C in sterile distilled water until use. One myrosinase unit (U) is defined as the amount of enzyme that can hydrolyse 1 μmol sinigrin per min at a pH of 6.5 at 37°C. A total of 500 mg of glucoerucin was hydrolysed in the presence of 25 U of myrosinase in 0.1 M potassium phosphate buffer, pH 6.5, for 2 hr at 37°C. ERU was extracted three times with 50 ml dichloromethane using a 250 ml separating funnel. The collected organic phases were unified and concentrated at 37°C by a rotary evaporator under vacuum. The obtained solution was dried using anhydrous Na<sub>2</sub>SO<sub>4</sub> and filtered, and the remaining dichloromethane was evaporated under a weak current of nitrogen. ERU was finally identified by GC-MS analysis on a Bruker GC 451 gas chromatograph equipped with an HP-5 fused silica capillary column (30 m by 0.25 mm inside diameter; 0.25 μm film thickness, J&W Scientific Inc, Folsom, California) connected to a quadrupole mass detector (Bruker Scion SQ Premium, Bruker Daltonics, Macerata, Italy). The oven temperature was set at 60°C and maintained for 4 min. Then, the temperature was programmed to rise from 60°C to 220°C at a rate of 10°C min<sup>-1</sup> and was finally held at 220°C for 4 min. The transfer line was maintained at 280°C, and the ion source was maintained at 220°C. Split injection (1:20) was applied, and the carrier gas flow (helium) was

set at 1 ml min<sup>-1</sup>. The mass spectrometer was operated in electron impact mode at 70 eV, scanning the range of 10–250 *m/z*, in a full scan acquisition mode. Mass spectra were identified by matching the recorded mass spectra with the NIST/EPA/NIH Mass Spectral Database (NIST 11, Gaithersburg, Maryland). A dichloromethane solution containing 0.2 mg/ml ERU and BITC (Sigma Aldrich 89983) as an internal standard was analysed to estimate the purity of the final natural ERU preparation. A response coefficient of 1.67 was calculated by the ratio of the slope of the calibration curves of BITC (Sigma Aldrich 89983) and of ERU (Santa Cruz sc-204741) dichloromethane solutions in the concentration range of 0.05 ÷ 1 mg/ml.

## 2.2 | Cell culture and cell viability assay

The human pancreas adenocarcinoma ascites metastasis cell line AsPC-1 (Sigma-Aldrich, passage number 3, population doubling time 38–40 hr) was cultured in RPMI 1640 (Sigma-Aldrich) supplemented with 2 mM glutamine (Sigma-Aldrich), 1 mM sodium pyruvate (Sigma-Aldrich), 10% foetal bovine serum (Sigma-Aldrich), and 1% of 100 units/ml penicillin and 100 mg/ml streptomycin (Sigma-Aldrich) in tissue culture flasks at 37°C in a humidified atmosphere and 5% CO<sub>2</sub>.

AsPC-1 cells were seeded onto 96-well plates at a density of 10<sup>4</sup> cells per well. After 24 hr, to allow cell attachment, the medium was replaced in each 96-well plate, and the cells were treated for 72 hr with ERU at the concentrations of 100, 30, 10 μM, or vehicle (dimethyl sulfoxide [DMSO] 1%). At the end of each treatment, cell viability was assessed using the cell proliferation reagent WST-1 (Roche, Basel, Switzerland; Citi et al., 2018), which is cleaved to formazan in living cells. WST-1 was added at a ratio of 1:10 of the total volume of the wells, and after 60 min of incubation at 37°C, the absorbance was measured at 450 nm by a multiplate reader (Enspire, Perkin-Elmer, Waltham, Massachusetts, United States).

## 2.3 | Evaluation of H<sub>2</sub>S release in AsPC-1 cells

The evaluation of H<sub>2</sub>S release into the cytosol of AsPC-1 cells was assessed by the spectrofluorometric method as previously described (Barresi et al., 2017). Briefly, AsPC-1 cells were cultured up to approximately 90% confluence, and 24 hr before the experiment, cells were seeded onto a 96-well black plate at a density of 72 × 10<sup>3</sup> cells per well.

After 24 hr, the cells were preloaded with a 100 μM solution of the fluorescent dye WSP-1 (Washington State Probe-1, Cayman Chemical; Liu et al., 2011). WSP-1 was first incubated with AsPC-1 cells for 30 min (allowing cells to upload the dye), then the supernatant was removed and replaced with a solution of the compounds to be tested, a reference drug or vehicle (dimethyl sulfoxide, DMSO 1%). The well-known H<sub>2</sub>S-releasing agent diallyl disulfide (DADS; Benavides et al., 2007; Liang, Wu, Wong, & Huang, 2015) was selected as a reference drug because it shows some physiochemical similarities to ERU (relatively low molecular weight, no charge, lipophilicity). The tested compound ERU, at the following concentrations 10, 30, and 100 μM and DADS 100 μM were first dissolved in DMSO and then diluted in buffer standard. This range of concentrations was selected on the basis of the anticancer concentrations found in the

literature for several ITCs (Su et al., 2015). When WSP-1 reacts with H<sub>2</sub>S, it releases a fluorophore detectable by a spectrofluorometer at λ = 465–515 nm (Peng et al., 2014). The increase in fluorescence (expressed as fluorescence index = FI) was monitored for 45 min using a spectrofluorometer (EnSpire, Perkin Elmer).

## 2.4 | Wound healing assay

AsPC-1 cells (4 × 10<sup>5</sup> cells per well) were plated in six-well tissue culture plates and grown to 90–95% confluence. After aspirating the medium, the centres of the cell monolayers were scraped with a 200 μl pipette tip to create a denuded zone (gap) of consistent width. Then, cellular debris was washed with phosphate buffer solution (PBS), and cells were treated with ERU at concentrations of 10 and 30 μM. The wound closure was monitored and photographed every 24 hr for 72 hr with an Olympus inverted microscope and camera (4x zoom). The gap was measured with ImageJ software.

## 2.5 | Analysis of cell cycle, caspase 3/7 activity, mitochondrial potential, and ERK1/2 phosphorylation

### 2.5.1 | General conditions

AsPC-1 cells were seeded, and after 24 hr, to allow cell attachment, the medium was replaced, and the cells were treated for 72 hr with 30 μM ERU, 10 μM Paclitaxel (positive control for caspase 3/7 activity), or vehicle (DMSO 1%) or were not treated.

### 2.5.2 | Cell cycle assay

The distribution of the cell cycle was analysed by flow cytometry using the Muse™ Cell Cycle Kit from EMD Millipore Bioscience. Cell cycle analysis was performed according to the manufacturer's protocol. AsPC-1 cells were seeded into 6-well plates at a density of 5 × 10<sup>5</sup> cells per well, and after incubation with the treatments (see general conditions), the cells were washed with PBS, detached, and fixed with 1 ml ice-cold 70% ethanol at –20°C for at least 3 hr. The cells were then washed with PBS, and 1 × 10<sup>6</sup> cells were stained with 200 μL of muse cell cycle reagent for 30 min at 37°C in the dark. Then, the cells were analysed by the Muse™ Cell Analyzer.

### 2.5.3 | Caspase 3/7 activity

Caspase 3/7 activity was analysed by flow cytometry using the Muse™ Caspase 3/7 Activity Kit from EMD Millipore Bioscience. Caspase 3/7 activity was evaluated according to the manufacturer's protocol. AsPC-1 cells were seeded into 24-well plates at a density of 1 × 10<sup>5</sup> cells per well, and after incubation with the treatments (see general conditions), the cells were detached, washed with PBS, and resuspended at a concentration of 1 × 10<sup>5</sup> to 5 × 10<sup>6</sup> cells/ml in the 1X assay buffer provided. Subsequently, 5 μl of Muse™ Caspase-3/7 Reagent working solution was added to 50 μl of cell suspension and incubated at 37°C for 30 min. Then, 150 μl of Muse™ Caspase 7-AAD working solution was added and incubated at 37°C for 5 min protected from light; cells were analysed by the Muse™ Cell Analyzer.

## 2.5.4 | Analysis of mitochondrial potential

Mitochondrial potential was analysed by flow cytometry using the Muse™ MitoPotential Assay Kit from EMD Millipore Bioscience. The mitochondrial potential was evaluated according to the manufacturer's protocol. AsPC-1 cells were seeded onto 24-well plates at a density of  $5 \times 10^5$  cells per well, and after incubation with the treatments (see general conditions), the cells were detached and resuspended at a concentration of  $1 \times 10^5$  cells/ml in the 1X assay buffer provided. Then, 95  $\mu$ l of Muse™ MitoPotential working solution was added to 100  $\mu$ l of cell suspension and incubated at 37°C for 20 min protected from light. Then, 5  $\mu$ l of Muse™ 7-AAD working solution was added and incubated at 37°C for 5 min; cells were analysed by the Muse™ Cell Analyser.

## 2.5.5 | Analysis of ERK1/2 phosphorylation

ERK1/2 phosphorylation was analysed by flow cytometry using the Muse™ MAPK phosphorylation Assay Kit from EMD Millipore Bioscience.

ERK1/2 phosphorylation was evaluated according to the manufacturer's protocol. AsPC-1 cells were seeded onto 24-well plates at a density of  $5 \times 10^5$  cells per well, and after incubation with the treatments (see general conditions), the cells were detached and suspended in 500  $\mu$ l of 1X assay buffer for every  $10^6$  cells. Then, fixation buffer was added in equal parts to the cell suspension (1:1 ratio) and incubated for 5 min on ice. After centrifugation (300 g for 5 min), the supernatant was removed, and the cells were suspended in 1 ml ice-cold permeabilization buffer and incubated for 5 min on ice. After centrifugation (300 g for 5 min), the supernatant was removed, and the cells were suspended in 450  $\mu$ l of 1X assay buffer. Following the incubation of 5  $\mu$ l of anti-ERK1/2, PECy5 antibody to 90  $\mu$ l of cell suspension for 3 min in the dark at room temperature, 100  $\mu$ l of 1X assay buffer was added, and cells were centrifuged (300 g for 5 min) to

discard the supernatant. Cells were suspended in 200  $\mu$ l of 1X assay buffer and analysed by the Muse™ Cell Analyser.

## 2.6 | Statistical analysis

Experiments were performed in triplicate each in three replicates. All data were expressed as the mean  $\pm$  standard error; ANOVA (followed by Bonferroni post test, when required) and student's *t* test were selected for the statistical analysis.  $p < 0.05$  was considered representative of significant differences (software: GraphPad Prism 6.0).

# 3 | RESULTS

## 3.1 | Production of natural ERU

Natural ERU (0.146 g, 0.878 mmol, 84% yield) was recovered as a light-yellow oil from the myrosinase catalysed hydrolysis of glucoerucin (96% purity, 0.5 g, 1.042 mmol). GC-MS analysis revealed a 97% purity level based on weight of ERU and the presence of 5-(methylsulfanyl) pentanenitrile at 1.7% based on the total peak area (Figure 1).

## 3.2 | Fluorometric recording of intracellular H<sub>2</sub>S-release

In a previous study, we reported the ability of ERU and other isothiocyanates to release H<sub>2</sub>S in a cell-free amperometric assay (Citi et al., 2014). According to these data, ERU exhibited a profile of a slow H<sub>2</sub>S-donor able to increase the release of H<sub>2</sub>S in the presence of an excess of L-cysteine, which was added into the medium (PBS buffer, pH = 7.4) to mimic a biological environment, rich in thiol groups. In the current study, we found that ERU releases H<sub>2</sub>S also inside cells. In particular, in this experimental assay, the increase of H<sub>2</sub>S-release

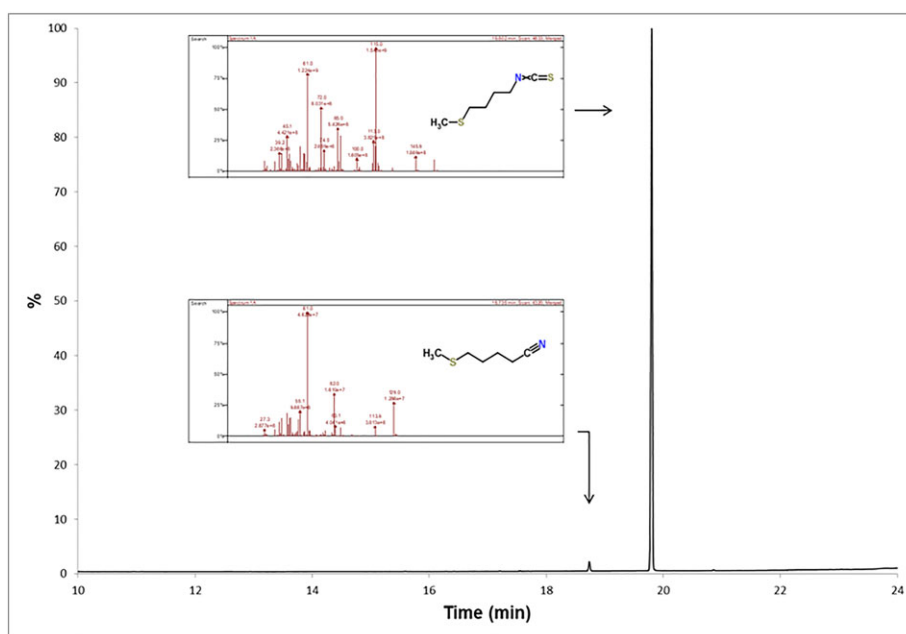


**FIGURE 1** GC chromatogram, MS spectra, and chemical structure of erucin (ERU). GC chromatogram and MS spectra (insert) of natural ERU purified after exogenous myrosinase hydrolysis of glucoerucin from *Eruca sativa* seeds [Colour figure can be viewed at [wileyonlinelibrary.com](http://wileyonlinelibrary.com)]

inside the AsPC-1 cell line was followed for 45 min until reaching the FI plateau (Figure 2a). The area under the curve (AUC) graph allows to better appreciate that ERU releases H<sub>2</sub>S in a concentration-dependent manner when administered to AsPC-1 cells at 10, 30, and 100 μM and that the highest concentration induces a H<sub>2</sub>S-release of approximately 40% of that of the natural reference H<sub>2</sub>S-donor DADS at the same concentration (Figure 2b).

### 3.3 | Cell viability

The results, expressed as a percentage of the value recorded for the vehicle-treated AsPC-1, showed a significant and concentration-dependent reduction of cell viability in cells treated for 72 hr with both 30 and 100 μM of ERU, whereas the 10 μM concentration did not evoke any inhibition. This ERU-induced inhibition of cell viability reached an efficacy value of approximately 90% at the highest concentration administered (100 μM) and a pIC<sub>50</sub> value of 4.43 ± 0.01 (Figure 2c).

### 3.4 | The ERU-induced inhibition of AsPC-1 cell migration

The inhibition of AsPC-1 cell migration induced by two different concentrations of ERU (10 and 30 μM) was assessed by a wound healing assay at 24, 48, and 72 hr. The 10 and 30 μM concentrations of ERU were selected because they showed submaximal effects on cell viability, and this feature made them more suitable for the wound healing assay than the 100 μM, which would cause a massive cell death. In

this assay, untreated cells exhibited a time-dependent wound healing rate recorded after 24, 48, and 72 hr (Table 1). Treatment with vehicle decreased the wound healing rate, but only after 24 hr, while after 48 and 72 hr, a recovery of wound healing rate percentage was observed (Table 1). Finally, treatment with ERU inhibited the migration of AsPC-1 cells in a concentration-dependent manner, at all timepoints (Figure 3a). In fact, wound healing ranges and migration rates were significantly decreased in AsPC-1 cells treated with 30 and 10 μM ERU (Figure 3b; Table 1).

### 3.5 | Inhibition of the cell cycle

After 72 hr of treatment with 30 μM ERU, a significant inhibition of AsPC-1 cell cycle progression was observed, with a particular increase of cells number in the G<sub>2</sub>/M phase (36.6% ± 3.5 vs. vehicle-treated cells in the G<sub>2</sub>/M phase: 24.0% ± 1.3) and in the S-phase (18.1% ± 1.5 vs. vehicle-treated cells in the S phase: 11.0% ± 0.7) and a consequent significant reduction of cells in the G<sub>0</sub>/G<sub>1</sub> phase (35.1% ± 5.0 vs. vehicle-treated cells in the G<sub>0</sub>/G<sub>1</sub> phase: 59.5% ± 1.8; Figure 4). Significant effects on the cell cycle have already been observed in several cancer cell lines treated with natural isothiocyanates (Abbaoui et al., 2012).

### 3.6 | Proapoptotic effects of ERU

In this work, we also investigated the ability of ERU to induce mitochondrial depolarization (a marker of early apoptosis). As shown in the graph (Figure 5d), 72 hr of treatment with 30 μM ERU, induced

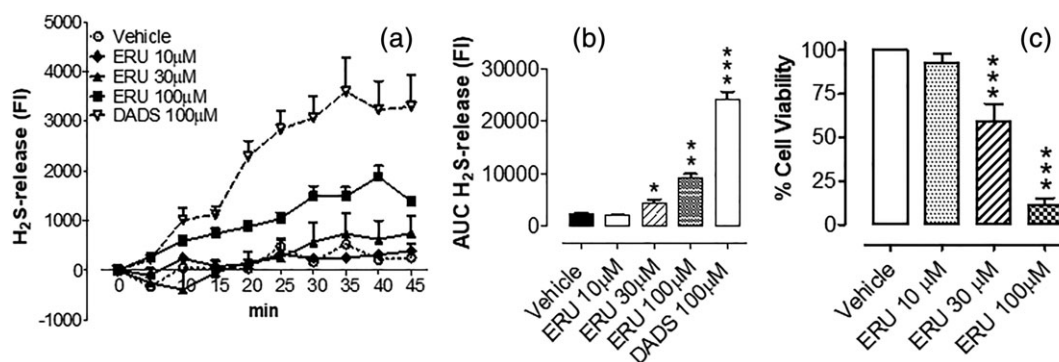


**FIGURE 2** Fluorometric recording of erucin (ERU)-mediated H<sub>2</sub>S release inside AsPC-1 cells and inhibition of cell viability induced by ERU in AsPC-1 cells after 72 hr of incubation. (a) Fluorometric recordings of H<sub>2</sub>S released by vehicle, 10, 30, and 100 μM ERU and 100 μM DADS for 45 min: The increase in H<sub>2</sub>S is expressed as fluorescence index. (b) The histograms show the total amount of H<sub>2</sub>S released by vehicle, 10, 30, and 100 μM ERU and 100 μM DADS during 45 min, expressed as AUC. (c) The histograms show the viability of AsPC-1 cells treated with vehicle or 10, 30, and 100 μM ERU. Data are expressed as a percentage of the value of absorbance recorded for AsPC-1 cells treated with vehicle. The vertical bars represent the standard error ( $n = 9$ ). The asterisks indicate a statistically significant difference from vehicle (\* $p < 0.05$ , \*\* $p < 0.01$ , \*\*\* $p < 0.001$ )

**TABLE 1** The table shows the percentages of the wound range recorded at T<sub>0</sub>, evoked by vehicle or erucin 10 and 30 μM after 24, 48, and 72 hr of incubation. Data are expressed as mean ± SEM

	Control (%)	Vehicle (%)	ERU 10 μM (%)	ERU 30 μM (%)
T24	57.0 ± 1.7	18.3 ± 4.1	19.3 ± 4.6	-11.2 ± 5.2
T48	92.2 ± 3.5	80.1 ± 2.3	27.1 ± 5.8	-22.1 ± 1.7
T72	98.0 ± 1.5	87.6 ± 3.7	57.5 ± 4.3	-0.1 ± 5.8

Note. ERU: erucin.



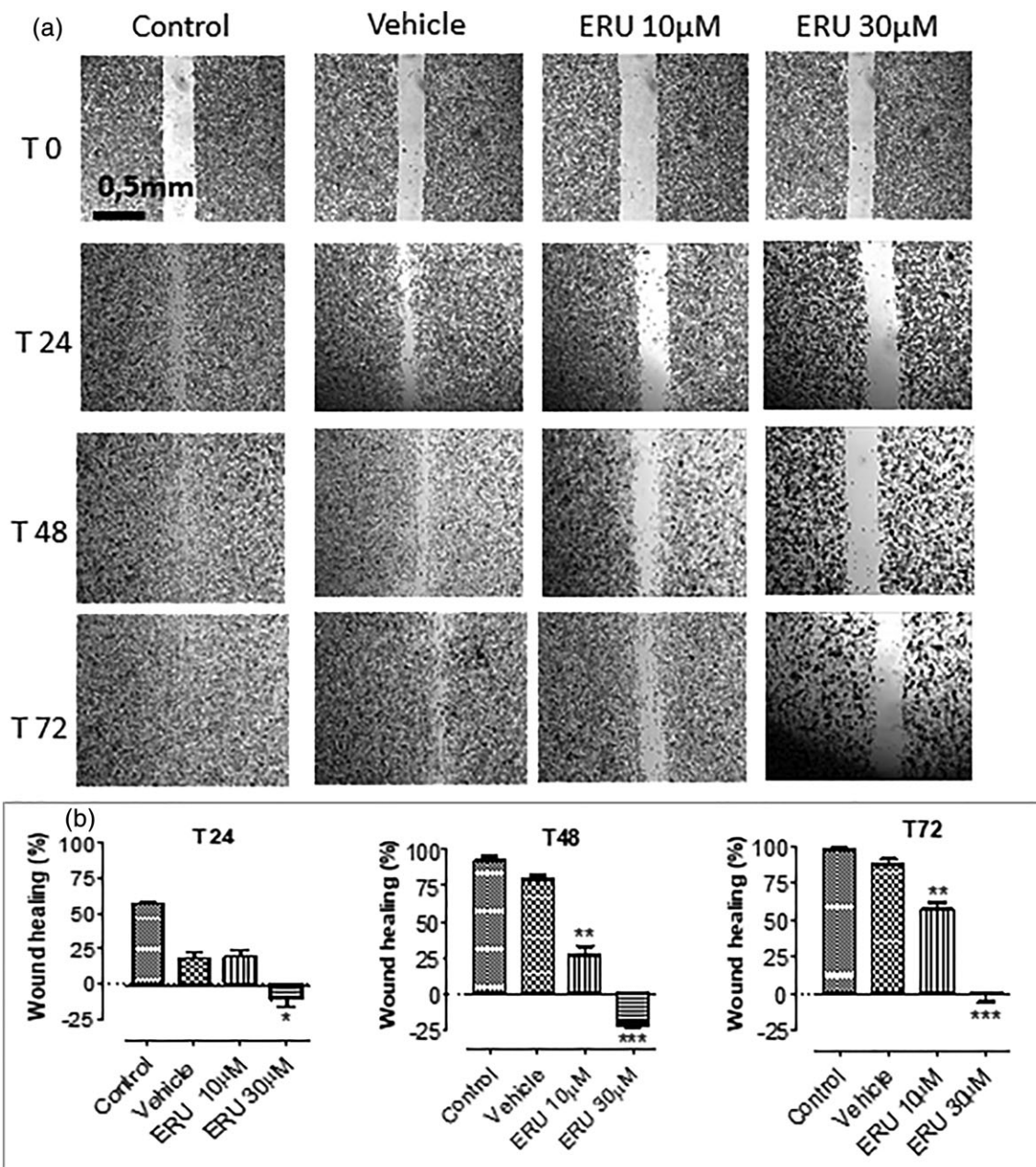


**FIGURE 3** The inhibition of cell migration assessed by a wound healing assay at 24, 48, and 72 hr. (a) The inhibition of cell migration was observed in the pictures obtained through the wound healing technique. The effects of vehicle, 10 and 30 µM ERU were observed after 0, 24, 48, and 72 hr of incubation. Pictures were obtained with a 4x objective. (b) The histograms represent the recovery of the wound range, expressed as a percentage of the wound range recorded at T0, evoked by vehicle or 10 and 30 µM ERU after 0, 24, 48, and 72 hr of incubation. The vertical bars represent the standard errors ( $n = 9$ ). The asterisks indicate a statistically significant difference from the value of the T0 wound range (\* $p < 0.05$ , \*\* $p < 0.01$ , \*\*\* $p < 0.001$ )

a decrease in live cells (vehicle:  $78.2\% \pm 4.5$  vs. ERU:  $60.0\% \pm 5.0$ ) and a significant increase in mitochondrial depolarization in both live cells (vehicle:  $7.3\% \pm 2.6$  vs. ERU:  $20.8\% \pm 4.1$ ) and dead cells (vehicle:  $12.9\% \pm 1.5$  vs. ERU:  $17.8\% \pm 1.9$ ). The increase of mitochondrial depolarization in cells treated with ERU is even more evident in graph 7B, in which the whole percentage of mitochondrial depolarization (in both live and dead cells) is shown (vehicle:  $20.3\% \pm 4.1$  vs. ERU:  $42.9\% \pm 2.5$ ; Figure 5e).

In this study, we also investigated a mild stage of apoptosis by evaluating the effect of ERU treatment on the increase in a well-known marker of apoptosis, caspase 3/7, in AsPC-1 cells after 72 hr

of treatment. Recording the caspase 3/7 levels, we obtained a graph in which we have four different states of cells: live, apoptotic live, apoptotic dead, and dead. In graph 8A, the effect of ERU on caspase 3/7 was compared with the effect of a well-known chemotherapeutic proapoptotic drug, paclitaxel at a concentration of 10 µM. After 72 hr, both 30 µM ERU and paclitaxel caused a significant reduction in the number of live cells (vehicle:  $78.4\% \pm 1.3$  vs. ERU:  $61.9\% \pm 1.3$  vs. paclitaxel:  $62.0\% \pm 1.0$ ), and treatment with paclitaxel resulted in an increase in the number of apoptotic cells, which was statistically significant both for apoptotic live (vehicle:  $8.1\% \pm 1.1$  vs. paclitaxel:  $13.0\% \pm 1.0$ ) and apoptotic dead cells (vehicle:  $9.6\% \pm 1.4$  vs.

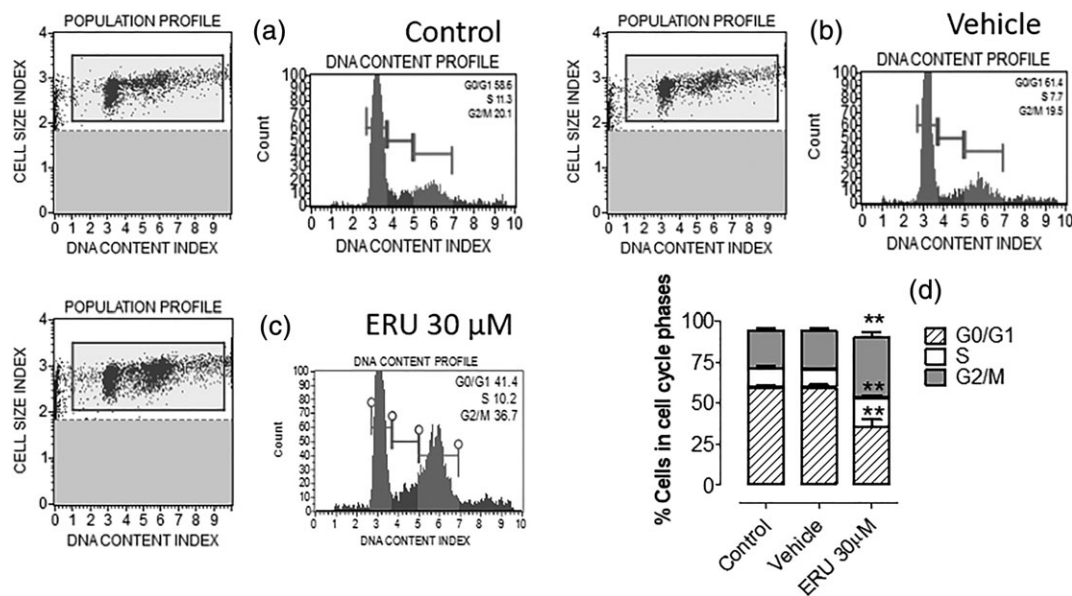


**FIGURE 4** Inhibition of cell cycle progression after 72 hr. A, b, c: typical cell cycle profiles of AsPC-1 cells with no treatment (a), after treatment with vehicle (b), and after treatment with 30 μM ERU (c). D: The histograms indicate the percentage of AsPC-1 cells in G0/G1, S, and G2/M cell cycle phases with no treatment (control), treatment with vehicle and 30 μM ERU, after 72 hr of incubation. The vertical bars represent the standard errors ( $n = 9$ ). The asterisks indicate a statistically significant difference from the percentage of AsPC-1 cells in different cell cycle phases after 72 hr of treatment with vehicle (\*\* $p < 0.01$ )

paclitaxel:  $16.6\% \pm 0.9$ ). For ERU, the effect was significant only for apoptotic dead cells (ERU:  $20.4\% \pm 2.0$ ; Figure 5). Overall, both 30 μM ERU and 10 μM paclitaxel (the positive control) significantly increased the number of total apoptotic cells (apoptotic dead cells and apoptotic live cells; vehicle:  $17.7\% \pm 2.5$  vs. ERU:  $28.7\% \pm 4.2$  vs. paclitaxel:  $29.1\% \pm 0.5$ ), suggesting a relevant role of the proapoptotic activity of ERU (Figure 5m).

### 3.7 | ERK1/2 phosphorylation in AsPC-1 cells

The MAPK/ERK pathway represents a fundamental step in cell proliferation, growth, and survival, and, as recently observed for other natural isothiocyanates, the inhibition of ERK phosphorylation represents a key target to suppress cancer cell proliferation (Jeong et al., 2017). Our data, obtained by recording the percentage of total ERK1/2 and phosphorylated ERK1/2 in AsPC-1 cells treated for 72 hr with vehicle or 30 μM ERU, showed reduced levels of phosphorylated ERK1/2 (vehicle:  $69.2\% \pm 2.4$  vs. ERU:  $56.3\% \pm 3.5$ ), suggesting a possible mechanism of action for the antiproliferative effect observed in the previous experiments (Figure 6a–c).

## 4 | DISCUSSION

Natural isothiocyanates have been known for their anticancer and chemopreventive effects (Jeon, Yoo, Jang, Jang, & Nam, 2011). Among natural isothiocyanates, the most studied is SFN, which is present in *Brassica oleracea* L. var. *italica* (broccoli), in particular, and few other species. ERU is a close analogue of SFN and is the isothiocyanate that is most present in rocket salad species, particularly in *E. sativa* Mill. seeds, in which its content is commonly close to 100 μmol/g (Lazzeri, Errani, Leoni, & Venturi, 2004). In the human body, ERU can also be

found as a metabolite derived from the *in vivo* reduction of SFN (Melchini & Traka, 2010). Among the several mechanisms of action proposed for the chemopreventive and anticancer properties of isothiocyanates, a recent observation of SFN was very promising: At low concentrations (1–5 μM), SFN was able to promote cell proliferation, whereas at high concentrations (10–40 μM), SFN inhibited cell proliferation, cell migration, and angiogenesis in several cancer types (Bao, Wang, Zhou, & Sun, 2014). This particular behaviour is called “hormesis,” which has also been used to describe the endogenous gasotransmitter hydrogen sulfide (Hellmich et al., 2015). Recently, our research group demonstrated that isothiocyanates, including natural isothiocyanates derived from *Brassicaceae* such as ERU, are real H<sub>2</sub>S donors that are able to increase their release of H<sub>2</sub>S in environments rich in free thiol groups such as biological environments (for instance, the cell cytosol; Citi et al., 2014; Martelli et al., 2014).

Natural isothiocyanates showed anticancer and chemopreventive properties with hormetic behaviour. Our group has already demonstrated that the natural isothiocyanate ERU exhibits hydrogen sulfide-releasing properties, and, because there is an intriguing overlap in the anticancer effect of isothiocyanates and H<sub>2</sub>S, in this work, we evaluated the anticancer properties of the natural isothiocyanate ERU on one of the most aggressive pancreatic adenocarcinoma cell lines (AsPC-1).

The first investigation was aimed at detecting the ability of ERU to release H<sub>2</sub>S inside AsPC-1 cells, thus showing the ability to cross the AsPC-1 cell membrane and release H<sub>2</sub>S at the intracellular level. As clearly highlighted in the experiments carried out with the fluorometric dye WSP-1, ERU was able to release H<sub>2</sub>S inside cells in a concentration-dependent manner, and this observation led to the conclusion that ERU acts as a H<sub>2</sub>S donor at the intracellular level. Exogenous H<sub>2</sub>S exhibits antiproliferative effects in different cancer cell lines (Ma et al., 2018). Consistently, the anticancer effects of slow

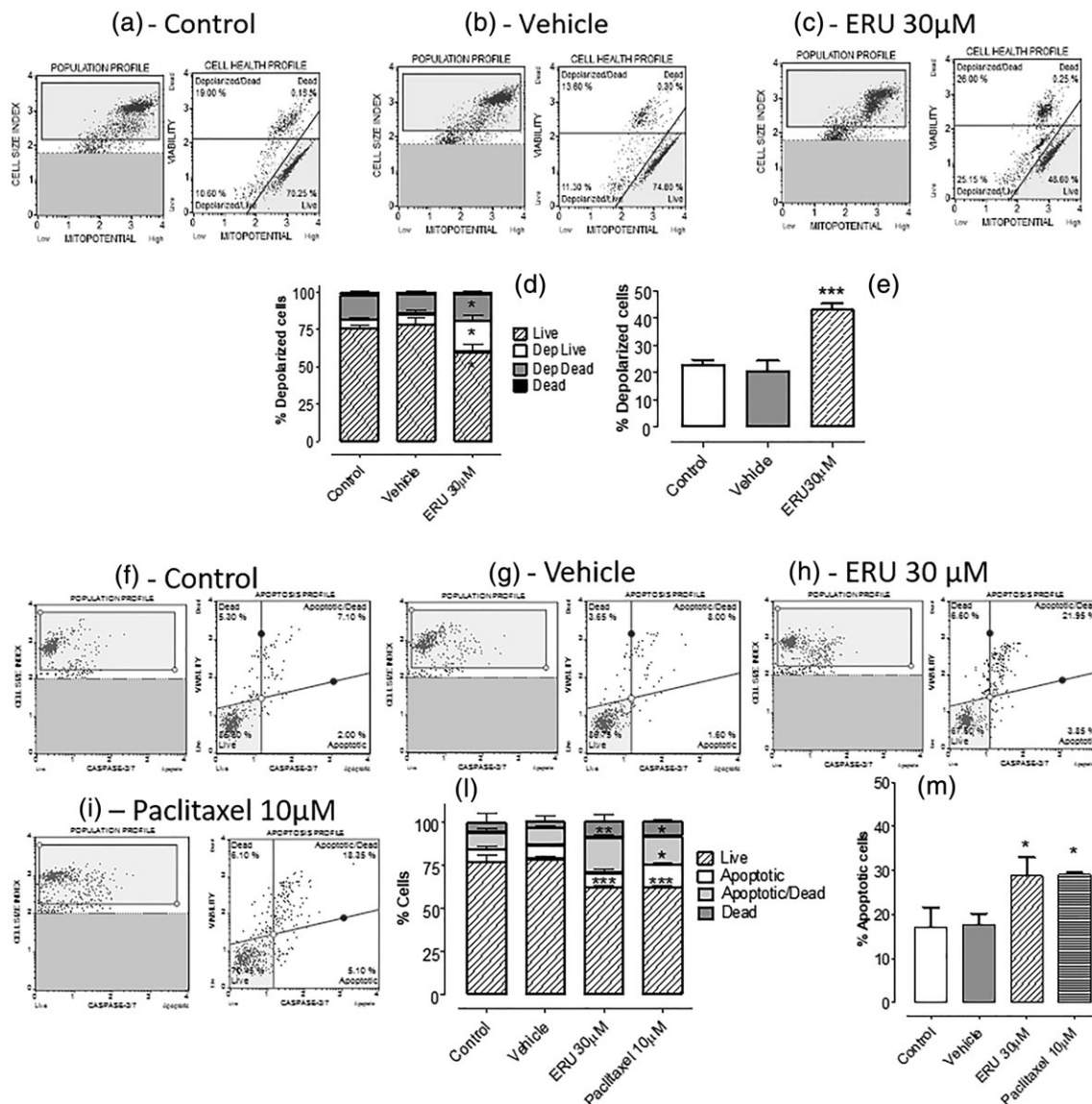


**FIGURE 5** The effect of erucin (ERU) on early (mitochondrial depolarization) and mild (caspase 3/7 levels) apoptosis in AsPC-1 cells after 72 hr of treatment. A, B, C: typical mitochondrial depolarization profiles of AsPC-1 cells with no treatment (a), after treatment with vehicle (b), and after treatment with 30  $\mu$ M ERU (c). (d) Early apoptosis was recorded as mitochondrial depolarization of AsPC-1 cells after 72 hr of no treatment (control), treatment with vehicle or 30  $\mu$ M ERU. For each treatment, four different states of mitochondrial depolarization were examined and reported as a percentage of the total number of cells: live, live with mitochondrial depolarization, dead with mitochondrial depolarization, and dead. (e) When the mitochondrial depolarization of live and dead cells was grouped, a higher significance was observed between AsPC-1 cells treated with vehicle or 30  $\mu$ M ERU. F, G, H, I: typical apoptotic profiles of AsPC-1 cells with no treatment (f), after treatment with vehicle (g), after treatment with 30  $\mu$ M ERU (h), and after treatment with 10  $\mu$ M paclitaxel (i). (l) Mild apoptosis was recorded as an increase in caspase 3/7 levels in AsPC-1 cells after 72 hr of no treatment (control), treatment with vehicle, treatment with 30  $\mu$ M ERU, or treatment with 10  $\mu$ M paclitaxel. For each treatment, four different states of cell apoptosis were examined and reported as a percentage of the total number of cells: live, apoptotic live, apoptotic dead, and dead. The vertical bars represent the standard errors ( $n = 9$ ). The asterisks indicate a statistically significant difference from the percentage of AsPC-1 cells in different degrees of apoptosis after the 72 hr of treatment between vehicle-, ERU-treated cells, or paclitaxel-treated cells (\* $p < 0.05$ , \*\* $p < 0.01$ , and \*\*\* $p < 0.001$ )

H<sub>2</sub>S-donors, such as GYY4137 (one of the pioneer compounds of this class), have been reported; GYY4137, a hydrogen sulfide (H<sub>2</sub>S) donor, shows potent anti-hepatocellular carcinoma activity by blocking the STAT3 pathway (Lu, Gao, Huang, & Wang, 2014). Even other natural H<sub>2</sub>S donors, such as acetyl deacylase disulfide, have been reported to promote H<sub>2</sub>S-mediated anticancer effects (De Cicco et al., 2017). On the basis of these premises, we hypothesize that the H<sub>2</sub>S-releasing effects of ERU could be a reasonable mechanism for its anticancer effects. Consistently in this work, 72 hr of incubation with ERU

produced a concentration-dependent inhibition of AsPC-1 cell viability with a pIC<sub>50</sub> value of  $4.43 \pm 0.01$ . In addition to the antiproliferative effect, ERU also significantly inhibited AsPC-1 migration. The AsPC-1 cell line, derived from ascitic metastasis of an adenocarcinoma of the head of the pancreas, represents a reliable model to verify the anti-migration properties of ERU. The reduction of wound healing was greatly impaired by ERU in a concentration-dependent manner. The concentration of 30  $\mu$ M ERU could evoke an almost maximal effect, leading to an almost full abolishment of AsPC-1 cell migration.



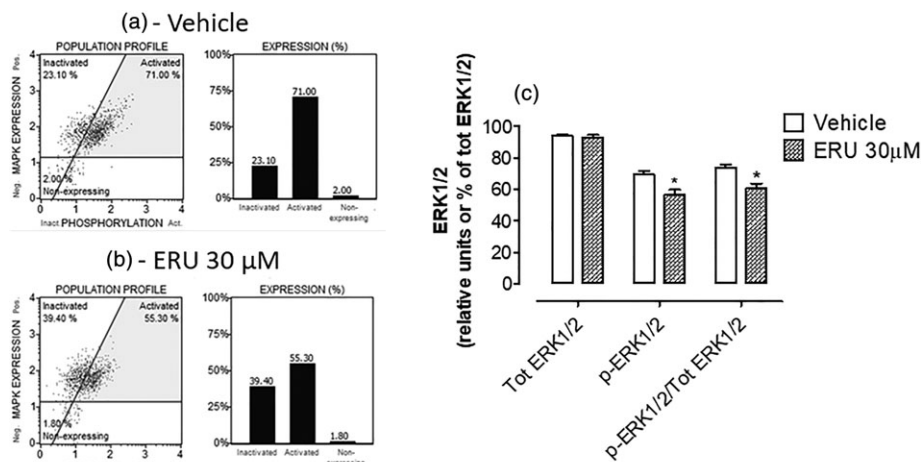


**FIGURE 6** p-ERK1/2 in AsPC-1 cells after 72 hr of treatment with erucin (ERU). A, b: typical ERK1/2 phosphorylation profiles of AsPC-1 cells after treatment with vehicle (a) and after treatment with 30 μM ERU (b); the % of inactivated cells indicates the nonphosphorylated ERK1/2 levels, the % of activated cells indicates the p-ERK1/2 levels, and the % of nonexpressing cells indicates cells not expressing ERK1/2. (c) The action of a 72 hr treatment with 30 μM ERU on the MAPK/ERK pathway of AsPC-1 cells was recorded, and the amount of total ERK1/2, phosphorylated ERK1/2, and the ratio between phosphor-ERK1/2 and total-ERK1/2 were calculated comparing the ERU-treated and vehicle-treated cells. The vertical bars represent the standard errors ( $n = 9$ ). In the second set of histograms, the asterisks indicate a statistically significant difference compared with the percentage of phosphorylated ERK1/2 in vehicle-treated AsPC-1 cells after 72 hr ( $*p < 0.05$ ). In the third set of histograms, the asterisks indicate a statistically significant difference compared with the percentage of the phosphor-ERK1/2/total-ERK1/2 ratio in vehicle-treated AsPC-1 cells after 72 hr ( $*p < 0.05$ )

This property of ERU has great importance in counteracting the metastatic process of particularly aggressive cancers, such as pancreatic adenocarcinoma. As already shown for other isothiocyanates and in other types of cancer, ERU demonstrated a clear ability to arrest the cell cycle in the G2/M phase and in the S phase, showing a consequent reduction of cells in the G0/G1 phase. This important property was coupled with another fundamental feature of a chemopreventive anticancer drug: ERU induced significant proapoptotic effects, which emerged when observing both early and mild stages of apoptosis. In fact, we recorded a marked increase in mitochondrial depolarization in AsPC-1 cells treated with ERU for 72 hr. We also found a significant increase in caspase 3/7 levels as a marker of cell apoptosis after ERU incubation for 72 hr. For the final investigation, we focused on the phosphorylation status of ERK1/2. In fact, pancreatic cancer cell lines are characterized by frequent mutations in the *KRAS* (v-Ki-ras2 Kirsten rat sarcoma viral oncogene homologue) gene, and in particular, AsPC-1 cells showed a mutation in the 12 codon of *KRAS*. This mutation led to a hyperactivation of *KRAS* with a consequent hyperphosphorylation of the downstream kinases (Deer et al., 2010). On this basis, we investigated the effect of 72 hr of treatment with 30 μM ERU on the phosphorylation of ERK1/2 in AsPC-1 cells. ERU did not affect the expression of ERK1/2 but led to significantly lower levels of phosphorylated ERK1/2. Because ERK1/2 is involved in the regulation of cell proliferation and cell survival, this ERU-mediated effect may contribute to the anticancer activity of this isothiocyanate.

## 5 | CONCLUSIONS

This work delineates the chemopreventive and anticancer profile of ERU in pancreatic adenocarcinoma. Our group first described natural and synthetic isothiocyanates as molecules that are able to release H<sub>2</sub>S. In this study, we demonstrated that treatment with ERU promotes a

significant intracellular increase of this gasotransmitter in AsPC-1 cells. Moreover, high concentrations of ERU (30–100 μM) inhibited AsPC-1 cell viability. ERU also inhibited cell migration and altered the AsPC-1 cell cycle, reducing G0/G1 phase and increasing G2/M and S phases, demonstrating proapoptotic effects in the early and mild stages. Finally, ERU administration was associated with reduced levels of phosphorylated ERK1/2. This feature is particularly important in pancreatic AsPC-1 cells because AsPC-1 are characterized by an activating mutation in *KRAS* that determines the hyperphosphorylation of ERK1/2 kinase, leading to pancreatic cancer cell proliferation, growth, and survival. Despite the wide characterization of ERU anticancer activities in human pancreatic adenocarcinoma, this study did not include *in vivo* experiments on animal xenograft models. This aspect is interesting, has many implications, and will be the main topic of future work. In conclusion, these data highlight the interesting biological properties of ERU, which can pave the way to a potential pharmacological exploitation of this compound and its analogues and facilitate the development of intriguing perspectives for nutraceutical products derived from *E. sativa* Mill.

## ACKNOWLEDGEMENTS

Part of the work (isolation of natural ERU) has been supported by the project "SUSCACE Sistema Integrato di Tecnologie per la valorizzazione dei sottoprodotti della filiera del Biodiesel," financed by MiPAAF (D.M. 2419, 20/02/08).

## CONFLICT OF INTEREST

The authors declare no conflict of interest.

## ORCID

Lorenzo Di Cesare Mannelli <https://orcid.org/0000-0001-8374-4432>  
Alma Martelli <https://orcid.org/0000-0002-2090-7107>

## REFERENCES

- Abbaoui, B., Riedl, K. M., Ralston, R. A., Thomas-Ahner, J. M., Schwartz, S. J., Clinton, S. K., & Mortazavi, A. (2012). Inhibition of bladder cancer by broccoli isothiocyanates sulforaphane and erucin: Characterization, metabolism, and interconversion. *Molecular Nutrition & Food Research*, *56*(11), 1675–1687. <https://doi.org/10.1002/mnfr.201200276>
- Bao, Y., Wang, W., Zhou, Z., & Sun, C. (2014). Benefits and risks of the hormetic effects of dietary isothiocyanates on cancer prevention. *PLoS One*, *9*(12), e114764. <https://doi.org/10.1371/journal.pone.0114764>
- Barresi, E., Nesi, G., Citi, V., Piragine, E., Piano, I., Taliani, S., ... Martelli, A. (2017). Iminothioethers as hydrogen sulfide donors: From the gas transmitter release to the vascular effects. *Journal of Medicinal Chemistry*, *60*(17), 7512–7523. <https://doi.org/10.1021/acs.jmedchem.7b00888>
- Benavides, G. A., Squadrito, G. L., Mills, R. W., Patel, H. D., Isbell, T. S., Patel, R. P., ... Kraus, D. W. (2007). Hydrogen sulfide mediates the vasoactivity of garlic. *Proceeding of the National Academy of Science U S A*, *104*(46), 17977–17982. <https://doi.org/10.1073/pnas.0705710104>
- Calderone, V., Martelli, A., Testai, L., Citi, V., & Breschi, M. C. (2016). Using hydrogen sulfide to design and develop drugs. *Expert Opinion in Drug Discovery*, *11*(2), 163–175. <https://doi.org/10.1517/17460441.2016.1122590>
- Citi, V., Del Re, M., Martelli, A., Calderone, V., Breschi, M. C., & Danesi, R. (2018). Phosphorylation of AKT and ERK1/2 and mutations of PIK3CA and PTEN are predictive of breast cancer cell sensitivity to everolimus in vitro. *Cancer Chemotherapy and Pharmacology*, *81*(4), 745–754. <https://doi.org/10.1007/s00280-018-3543-6>
- Citi, V., Martelli, A., Testai, L., Marino, A., Breschi, M. C., & Calderone, V. (2014). Hydrogen sulfide releasing capacity of natural isothiocyanates: Is it a reliable explanation for the multiple biological effects of Brassicaceae? *Planta Medica*, *80*(8–9), 610–613. <https://doi.org/10.1055/s-0034-1368591>
- Clarke, J. D., Hsu, A., Riedl, K., Bella, D., Schwartz, S. J., Stevens, J. F., & Ho, E. (2011). Bioavailability and inter-conversion of sulforaphane and erucin in human subjects consuming broccoli sprouts or broccoli supplement in a cross-over study design. *Pharmacological Research*, *64*(5), 456–463. <https://doi.org/10.1016/j.phrs.2011.07.005>
- De Cicco, P., Panza, E., Armogida, C., Ercolano, G., Tagliatalata-Scafati, O., Shokoohinia, Y., ... Ianaro, A. (2017). The hydrogen sulfide releasing molecule acetyl deacylasadisulfide inhibits metastatic melanoma. *Frontiers in Pharmacology*, *8*, 65. <https://doi.org/10.3389/fphar.2017.00065>
- Deer, E. L., Gonzalez-Hernandez, J., Coursen, J. D., Shea, J. E., Ngatia, J., Scaife, C. L., ... Mulvihill, S. J. (2010). Phenotype and genotype of pancreatic cancer cell lines. *Pancreas*, *39*(4), 425–435. <https://doi.org/10.1097/MPA.0b013e3181c15963>
- Fofaria, N. M., Ranjan, A., Kim, S. H., & Srivastava, S. K. (2015). Mechanisms of the anticancer effects of isothiocyanates. *Enzyme*, *37*, 111–137. <https://doi.org/10.1016/bs.enz.2015.06.001>
- Franco, P., Spinozzi, S., Pagnotta, E., Lazzeri, L., Ugolini, L., Camborata, C., & Roda, A. (2016). Development of a liquid chromatography-electrospray ionization-tandem mass spectrometry method for the simultaneous analysis of intact glucosinolates and isothiocyanates in Brassicaceae seeds and functional foods. *Journal of Chromatography A*, *1428*, 154–161. <https://doi.org/10.1016/j.chroma.2015.09.001>
- Fuentes, F., Paredes-Gonzalez, X., & Kong, A. N. (2015). Dietary glucosinolates sulforaphane, phenethyl isothiocyanate, indole-3-carbinol/3,3'-diindolylmethane: Anti-oxidative stress/inflammation, Nrf2, epigenetics/epigenomics and in vivo cancer chemopreventive efficacy. *Current Pharmacology Reports*, *1*(3), 179–196. <https://doi.org/10.1007/s40495-015-0017-y>
- Hellmich, M. R., Coletta, C., Chao, C., & Szabo, C. (2015). The therapeutic potential of cystathionine beta-synthetase/hydrogen sulfide inhibition in cancer. *Antioxidant Redox Signal*, *22*(5), 424–448. <https://doi.org/10.1089/ars.2014.5933>
- Jeon, Y. K., Yoo, D. R., Jang, Y. H., Jang, S. Y., & Nam, M. J. (2011). Sulforaphane induces apoptosis in human hepatic cancer cells through inhibition of 6-phosphofructo-2-kinase/fructose-2,6-biphosphatase4, mediated by hypoxia inducible factor-1-dependent pathway. *Biochimica et Biophysica Acta*, *1814*(10), 1340–1348. <https://doi.org/10.1016/j.bbapap.2011.05.015>
- Jeong, Y. J., Cho, H. J., Chung, F. L., Wang, X., Hoe, H. S., Park, K. K., ... Chang, Y. C. (2017). Isothiocyanates suppress the invasion and metastasis of tumors by targeting FAK/MMP-9 activity. *Oncotarget*, *8*(38), 63949–63962. <https://doi.org/10.18632/oncotarget.19213>
- Lazzeri, L., Errani, M., Leoni, O., & Venturi, G. (2004). Eruca sativa spp. oleifera: A new non-food crop. *Industrial Crops and Products*, *20*(1), 67–73. <https://doi.org/10.1016/j.indcrop.2002.06.001>
- Lazzeri, L., Malaguti, L., Cinti, S., Ugolini, L., De Nicola, G. R., Bagatta, M., ... D'Avino, L. (2013). The Brassicaceae biofumigation system for plant cultivation and defence. An Italian twenty-year experience of study and application.
- Liang, D., Wu, H., Wong, M. W., & Huang, D. (2015). Diallyl trisulfide is a fast H<sub>2</sub>S donor, but diallyl disulfide is a slow one: The reaction pathways and intermediates of glutathione with polysulfides. *Organic Letters*, *17*(17), 4196–4199. <https://doi.org/10.1021/acs.orglett.5b01962>
- Liu, C., Pan, J., Li, S., Zhao, Y., Wu, L. Y., Berkman, C. E., ... Xian, M. (2011). Capture and visualization of hydrogen sulfide by a fluorescent probe. *Angewandte Chemie International Edition in English*, *50*(44), 10327–10329. <https://doi.org/10.1002/anie.201104305>
- Lu, S., Gao, Y., Huang, X., & Wang, X. (2014). GYY4137, a hydrogen sulfide (H<sub>2</sub>S) donor, shows potent anti-hepatocellular carcinoma activity through blocking the STAT3 pathway. *International Journal of Oncology*, *44*(4), 1259–1267. <https://doi.org/10.3892/ijo.2014.2305>
- Lucarini, E., Micheli, L., Trallori, E., Citi, V., Martelli, A., Testai, L., ... Di Cesare Mannelli, L. (2018). Effect of glucoraphanin and sulforaphane against chemotherapy-induced neuropathic pain: Kv7 potassium channels modulation by H<sub>2</sub>S release in vivo. *Phytotherapy Research*, *32*, 2226–2234. <https://doi.org/10.1002/ptr.6159>
- Ma, Y., Yan, Z., Deng, X., Guo, J., Hu, J., Yu, Y., & Jiao, F. (2018). Anticancer effect of exogenous hydrogen sulfide in cisplatinresistant A549/DDP cells. *Oncology Reports*, *39*(6), 2969–2977. <https://doi.org/10.3892/or.2018.6362>
- Martelli, A., Testai, L., Citi, V., Marino, A., Bellagambi, F. G., Ghimenti, S., ... Calderone, V. (2014). Pharmacological characterization of the vascular effects of aryl isothiocyanates: Is hydrogen sulfide the real player? *Vascular Pharmacology*, *60*(1), 32–41. <https://doi.org/10.1016/j.vph.2013.11.003>
- Melchini, A., & Traka, M. H. (2010). Biological profile of erucin: A new promising anticancer agent from cruciferous vegetables. *Toxins (Basel)*, *2*(4), 593–612. <https://doi.org/10.3390/toxins2040593>
- Nastruzzi, C., Cortesi, R., Esposito, E., Menegatti, E., Leoni, O., Iori, R., & Palmieri, S. (2000). In vitro antiproliferative activity of isothiocyanates and nitriles generated by myrosinase-mediated hydrolysis of glucosinolates from seeds of cruciferous vegetables. *Journal of Agricultural and Food Chemistry*, *48*(8), 3572–3575. <https://doi.org/10.1021/jf000191p>
- Panza, E., De Cicco, P., Armogida, C., Scognamiglio, G., Gigantino, V., Botti, G., ... Ianaro, A. (2015). Role of the cystathionine gamma lyase/hydrogen sulfide pathway in human melanoma progression. *Pigment Cell Melanoma Research*, *28*(1), 61–72. <https://doi.org/10.1111/pcmr.12312>
- Peng, B., Chen, W., Liu, C., Rosser, E. W., Pacheco, A., Zhao, Y., ... Xian, M. (2014). Fluorescent probes based on nucleophilic substitution-cyclization for hydrogen sulfide detection and bioimaging. *Chemistry*, *20*(4), 1010–1016. <https://doi.org/10.1002/chem.201303757>

- Pessina, A., Thomas, R. M., Palmieri, S., & Luisi, P. L. (1990). An improved method for the purification of myrosinase and its physicochemical characterization. *Archives of Biochemistry and Biophysics*, 280(2), 383–389. [https://doi.org/10.1016/0003-9861\(90\)90346-Z](https://doi.org/10.1016/0003-9861(90)90346-Z)
- Su, J. C., Lin, K., Wang, Y., Sui, S. H., Gao, Z. Y., & Wang, Z. G. (2015). In vitro studies of phenethyl isothiocyanate against the growth of LN229 human glioma cells. *International Journal of Clinical and Experimental Pathology*, 8(4), 4269–4276.

**How to cite this article:** Citi V, Piragine E, Pagnotta E, et al. Anticancer properties of erucin, an H<sub>2</sub>S-releasing isothiocyanate, on human pancreatic adenocarcinoma cells (AsPC-1). *Phytotherapy Research*. 2019;33:845–855. <https://doi.org/10.1002/ptr.6278>